Biomechanical effect of anatomical tibial component design on stress shielding of medial proximal tibial bone in total knee arthroplasty: finite element analysis of 30 Korean models

Byung Woo Cho

Department of Medicine

The Graduate School, Yonsei University

Biomechanical effect of anatomical tibial component design on stress shielding of medial proximal tibial bone in total knee arthroplasty: finite element analysis of 30 Korean models

Directed by Professor Kwan Kyu Park

The Doctoral Dissertation
submitted to the Department of Medicine,
the Graduate School of Yonsei University
in partial fulfillment of the requirements for the degree
of Doctor of Philosophy in Medical Science

Byung Woo Cho

December 2021

This certifies that the Doctoral Dissertation of Byung Woo Cho is approved.

Thesis Supervisor: Kwan Kyu Park

Thesis Committee Member#1: Hyuck Min Kwon

Thesis Committee Member#2: Kyoung-Tak Kang

Thesis Committee Member#3: Sung-Rae Cho

Thesis Committee Member#4: Sun Kook Yoo

The Graduate School
Yonsei University

December 2021

ACKNOWLEDGEMENTS

I thank Nayung Kim and Geonho Cho for their invaluable advice and unconditional support.

<TABLE OF CONTENTS>

LIST OF FIGURES

LIST OF TABLES

ABSTRACT

Biomechanical effect of anatomical tibial component design on stress shielding of medial proximal tibial bone in total knee arthroplasty: finite element analysis of 30 Korean models

Byung Woo Cho

Department of Medicine
The Graduate School, Yonsei University

(Directed by Professor Kwan Kyu Park)

Purpose

This study aimed to identify the effect of anatomical tibial component (ATC) design on stress distribution in the proximal tibia of Koreans using finite element analysis (FEA).

Materials and Methods

Three-dimensional (3D) finite element models of 30 tibias were created using modified tetrahedral ten-node elements. A symmetric tibial component (STC, NexGen LPS-Flex) and an ATC (Persona) were used in surgical simulation. We compared the FEA measurements (stress and strain) around the stem tip and in the medial half of the proximal tibial bone, as well as the distance from the distal stem tip to the shortest anteromedial cortical bone. Then, correlations between this distance and FEA measurements were analyzed.

Results

The distance from the distal stem tip to the shortest cortical bone showed no statistically significant difference between implants. However, the peak von Mises stress around the distal stem tip was higher with STC than with ATC. In the medial half of the proximal tibial bone, the peak von Mises stress showed no

statistical difference between two implants; but the average von Mises stress, maximum principal strain, and minimum principal strain were higher with ATC. Both implants showed a negative correlation between the distance and peak stress around the distal stem tip. In the medial half of the proximal tibial bone, ATC showed a positive correlation between the distance and average von Mises stress and a negative correlation between the distance and average minimum principal strain. STC showed no correlation between the distance and average values in the medial half of the proximal tibial bone.

Conclusion

Implant design, including the medialized stem and the anatomic shape of the baseplate, affects the distribution of stress and strain on the proximal tibia. In Korean women, the medialized stem of ATC does not come closer to the cortical bone and transmits more stress and strain to the proximal tibial bone than STC does. However, unlike STC, the shorter the distance between the stem and the anteromedial cortical bone, the less stress and strain applied to the medial proximal cutting plane in ATC. Therefore, when using ATC, stress shielding should be considered in patients with severe anatomical variations or in cases of surgical error.

Key words: total knee arthroplasty, finite element analysis, anatomical tibial component, stress shielding, medial proximal tibial bone loss

Biomechanical effect of anatomical tibial component design on stress shielding of medial proximal tibial bone in total knee arthroplasty: finite element analysis of 30 Korean models

Byung Woo Cho

Department of Medicine
The Graduate School, Yonsei University

(Directed by Professor Kwan Kyu Park)

I. INTRODUCTION

Total knee arthroplasty (TKA) shows excellent results in the treatment of end-stage knee osteoarthritis. With increased life span after TKA, interest in the longevity of artificial joints has increased, and various devices are being developed accordingly. Recently, an anatomical tibial component (ATC) that intends to enhance clinical outcomes has been introduced. This implant comprises a medialized stem (Fig. 1-A) and an anatomically shaped baseplate (Fig. 1-B), similar to the human tibia. Although this design is used worldwide, certain races and situations may show variations that differ from the manufacturer's expectations.

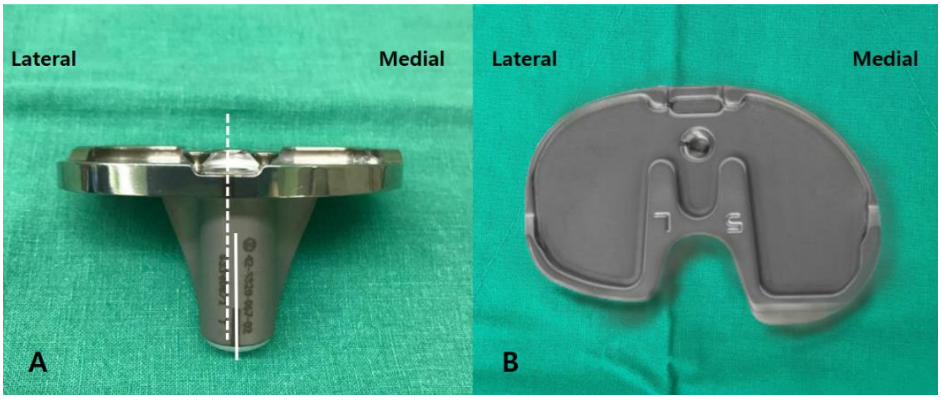

Figure 1. (A) Medialized stem and (B) asymmetric baseplate of an anatomical tibial component.

The tibial canal is biased medially in Caucasians[1,2], and ATC was designed to achieve optimal alignment with a medialized stem. However, in Asians, the tibial canal is biased anterolaterally from the center of the tibial plateau,[3] such that a medially offset stem can induce mismatched alignment[4], causing stress shielding and bone loss[5]. According to previous literature, there should be less bone loss with an ATC with a shorter stem, thinner baseplate, and more tibial plateau coverage, relative to conventional implants[6-8]. Cho *et al*. reported that ATC is more likely to induce medial tibial bone loss than a symmetric tibial component (STC) due to stress shielding in Korean patients[5]. Regarding this matter, they suggested that inefficient stress transfer due to a medialized stem may be one of the causes[5]. However, due to the inherent limitations of their retrospective observational study, a clear mechanism has not been identified.

Finite element analysis (FEA) is a computational procedure used for stress analysis of complex structures in the biomedical engineering field. It has been used in analyzing mechanical stimuli alterations according to the implant design, material, and surgical methods that affect stress shielding in total hip arthroplasty[9,10] and TKA[11,12]. In clinical practice, controlling factors that affect stress shielding of the bone around an implant is almost impossible. Therefore, it is believed that surgical simulation using FEA would help analyze stress shielding according to ATC characteristics.

The present study aimed to identify the effect of ATC design on stress distribution in the proximal tibias of Koreans using FEA. We hypothesized that an ATC with a medialized stem will have higher stress values between the stem distal tip and medial cortical bone compared to an STC, thereby reducing strain on the proximal tibial bone.

II. MATERIALS AND METHODS

1. Data collection

With approval from our institutional review board, 30 patients undergoing TKA

using an ATC (Persona, Zimmer, Warsaw, IN, USA) were retrospectively enrolled. Since the stem was 1–4 mm medialized, depending on the size of the tibial component, only patients with size D were enrolled. Preoperative computed tomography image data were stored in the Digital Imaging and Communications in Medicine (DICOM; National Electrical Manufacturers Association, Rosslyn, Virginia) format.

2. Finite element model and surgical simulation

The acquired DICOM data were imported into Mimics software (version 21.0; Materialize, Leuven, Belgium). In Mimics software, the marching squares algorithm is used for thresholding and segmenting anatomic structures of interest according to a predetermined grayscale value[13]. A well-trained technician segmented the areas of interest by applying manual and automated thresholding techniques to the raw DICOM data. An attending orthopedic doctor guided and supervised the technician.

Three-dimensional (3D) finite element models (FEMs) were created using modified tetrahedral ten-node elements with ABAQUS software (ABAQUS Inc., Providence, RI, USA). It was assumed that the tibial component and tibial bone were completely fixed. The isotropic material values (Young's modulus of elasticity and Poisson's ratio ν) were as follows: cancellous bone (0.7 GPa, 0.30), cortical bone (17 GPa, 0.30), cement (2.2 GPa, 0.46), and Ti6AL4V (110 GPa, 0.30)[14]. The thickness of the cortical bone and cement was set to 2 mm. The load was set to approximately 2,000 N, considering that thrice the load is applied in the late stance phase when a 70 kg adult walks. The load was divided into 7:3 ratios on the medial and lateral condyles, respectively[14-16]. A mesh convergence analysis of maximum displacement in the FEMs was assessed, similar to a previous study[17]. The convergence rate of maximum displacement was <0.1% in all models. The number of elements was as follows: tibial plate, 151,902; cement, 48,654; cortical bone, 293,444; and cancellous bone, 425,015.

The surgical simulation was performed as follows. The tibial shaft was defined as a line connecting the center between the tibial spines and the center of a sphere fitted to the talocrural joint. The proximal tibia was cut perpendicular to the tibial shaft with a posterior slope of 3°; the cutting level was set to 8 mm from the highest side of the tibial plateau (all lateral condyles in this study). During implant insertion, the anteroposterior position was aligned with the anterior border, and the mediolateral position was placed in the middle.

The rotation of tibial components was aligned to the line between the center of posterior cruciate ligament footprint and medial third of the tibial tubercle. An STC (NexGen LPS-Flex size 3) and ATC (Persona size D) from a single manufacturer (Zimmer, Warsaw, IN, USA) were used (Fig. 2). The specifications of these implants are presented in Table 1.

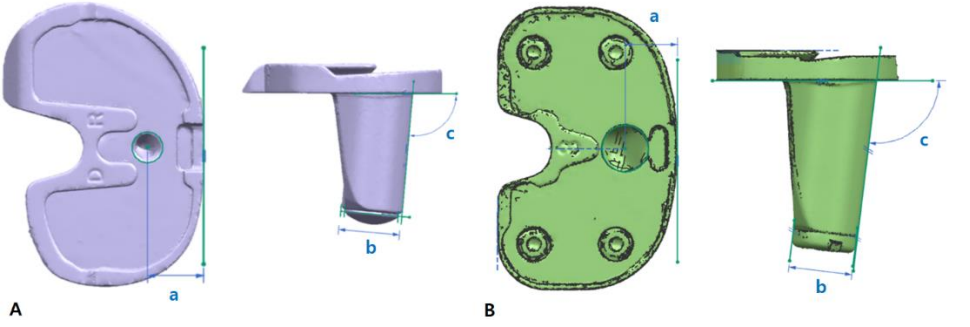

Figure 2. Baseplate shape and sagittal view of (A) ATC and (B) STC. a: Distance from anterior border to stem center at baseplate. b: Stem diameter at distal tip. c: Sagittal angle between stem axis and baseplate.

Table 1. Specifications of both implants

	ATC (Persona D)	STC (NexGen 3)
Baseplate medio-lateral length	67.1 mm	66.5 mm
Baseplate thickness	3.68 mm	4.18 mm
Stem length	31.4 mm	39.7 mm
Material	Titanium	Titanium
Sagittal angle between stem axis and baseplate	5°	7°
Stem diameter at distal tip (metal part)	14.2 mm	14.48 mm
Distance from anterior border to stem center at baseplate	13.05 mm	12.3 mm

ATC, anatomical tibial component; STC, symmetric tibial component.

3. Finite element model measurements

When each implant was inserted and load applied, the stress concentration and the risk of bone resorption around the distal stem tip and in the medial half of the proximal tibial bone were evaluated [14,18-20]. To evaluate the stress concentration around the stem distal tip and 5-mm thick medial half of proximal tibial bone, the peak von Mises stress among the cancellous bone elements was measured (Fig. 3). To evaluate the risk of bone resorption to the tibial cutting plane, the average von Mises stress and average principal strains of the 5-mm thick proximal medial half cancellous bone were measured.

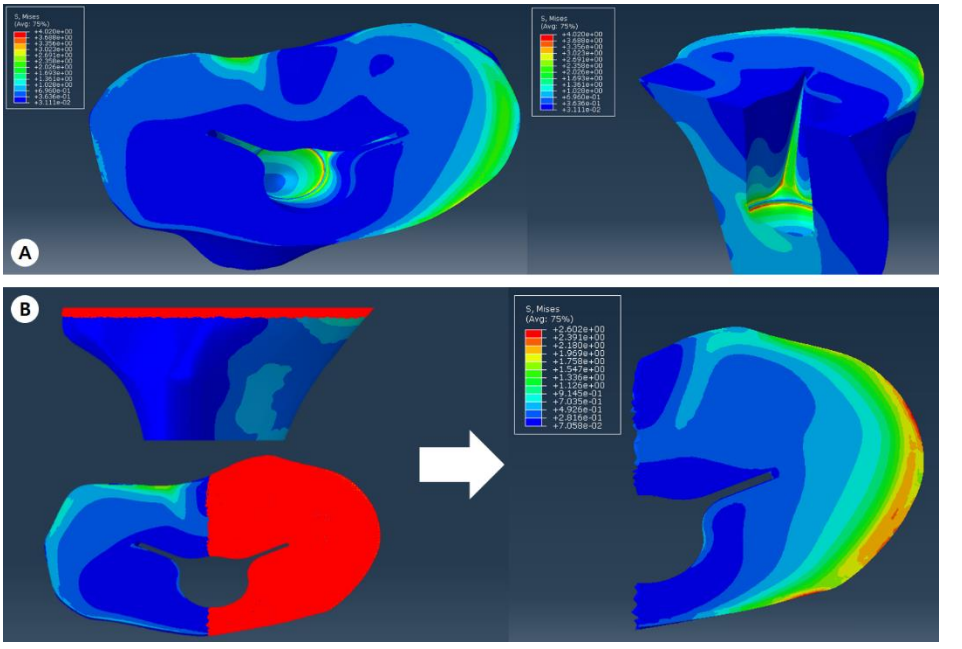

Figure 3. (A) Von Mises stress plot for cancellous bone around the distal stem tip. (B) Von Mises stress plot for the medial half of 5-mm thick proximal tibial bone.

When each implant was inserted, the distance from the distal stem tip to the shortest anteromedial cortical bone was measured and analyzed. The distance was measured on a plane perpendicular to the stem axis passing through the most distal part (Fig. 4). To evaluate intra- and inter-observer reliability of distance measurements, the models were evaluated by two blinded orthopedic surgeons at 4-week intervals.

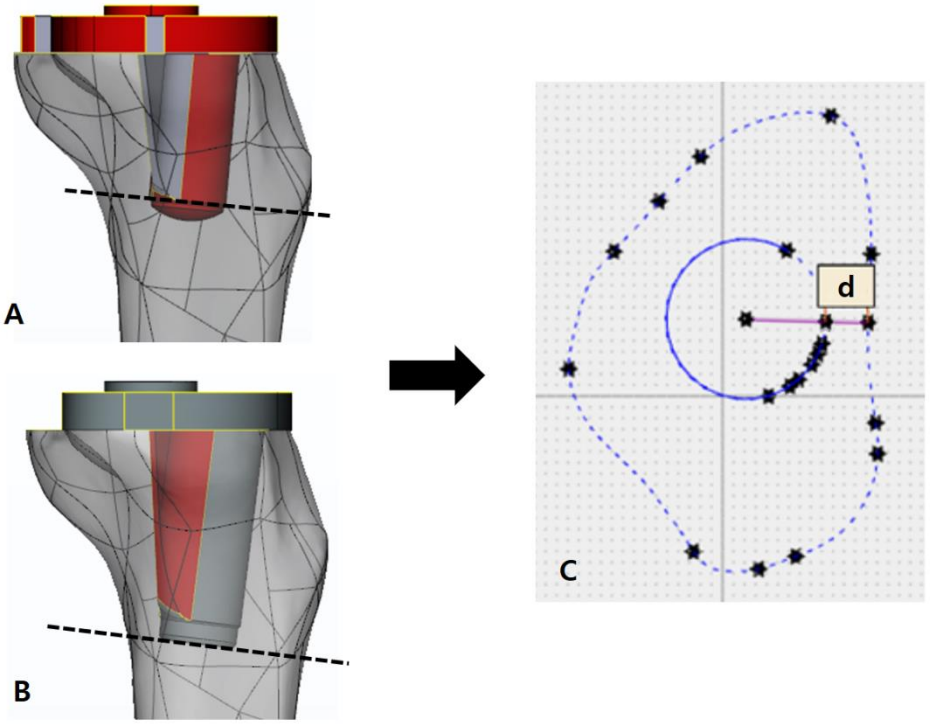

Figure 4. Surgical simulations of (A) ATC and (B) STC in the same patient. (C) The plane perpendicular to the stem axis at the most distal end. d: The shortest distance between distal stem tip and anteromedial cortical bone.

4. Statistical analysis

A paired t-test was performed to compare the differences in stress, strain, and distance according to implant type. Pearson correlation analysis was performed to evaluate the relationship between distance and FEA measurements. Statistical analysis was performed using SPSS statistical software (version 25.0, SPSS, Chicago, IL). Statistical significance was set at P <0.05. The intra- and inter-observer reliabilities of the measurements were assessed using intra-class correlation coefficients.

III. RESULTS

Patient demographics are shown in Table 2. All patients were female, and 15 knees (50%) were right-sided. The mean age was 71.2 ± 5.9 years (range 59–79 years); the mean height was 154.9 ± 4.7 cm (range 149.1–165.0 cm); and the mean body mass index was 27.3 ± 3.4 kg/m² (range 22.2–33.2 kg/m²).

Table 2. Patient demographics

	% or Mean ± SD	Range
Female sex (%)	100	-
Right knee (%)	50	-
Age (years)	71.2 ± 5.9	59 to 79
Height (cm)	154.9 ± 4.7	149.1 to 165.0
BMI (kg/m²)	27.3 ± 3.4	22.2 to 33.2

SD, standard deviation; BMI, body mass index.

Table 3 shows the stress, strain, and distance measurements when ATC and STC were inserted. The distance from the distal stem tip of the two implants to the shortest cortical bone showed no statistically significant difference (ATC 3.91 ± 1.07 mm and STC 3.91 ± 1.18 mm, p=0.979). However, the maximum von Mises stress near the distal stem tip was higher with STC than with ATC (5.52 ± 0.64 MPa and 4.41 ± 0.39 MPa, p<0.001). In the medial half of the proximal tibial bone, the peak von Mises stress showed no statistical difference between the two implants (ATC 2.66 ± 0.64 and STC 2.71 ± 0.61, p=0.247); but the average von Mises stress, maximum principal strain, and minimum principal strain were higher with ATC (ATC 0.453 ± 0.021 and STC 0.404 ± 0.017, p<0.001; ATC 305 ± 14 and STC 272 ± 9, p<0.001; ATC -622 ± 32 and STC -553 ± 29, p<0.001).

Table 3. Results of paired t-test between ATC and STC

	ATC	STC	
	Mean ± SD (range)	Mean ± SD (range)	p-value
Distance between stem tip and cortical bone (mm)	3.91 ± 1.07 (1.59 to 6.05)	3.91 ± 1.18 (1.13 to 5.61)	0.979
Around stem tip area			
Peak von Mises stress (MPa)	**4.41 ± 0.39 (3.70 to 5.47)**	**5.52 ± 0.64 (4.18 to 7.49)**	**<0.001**
Medial half of proximal tibial bone			
Peak von Mises stress (MPa)	2.66 ± 0.64 (1.83 to 4.39)	2.71 ± 0.61 (1.66 to 3.87)	0.247
Average von Mises stress (MPa)	**0.453 ± 0.021 (0.405 to 0.487)**	**0.404 ± 0.017 (0.373 to 0.428)**	**<0.001**
Average maximum principal strain (μstrain)	**305 ± 14 (282 to 335)**	**272 ± 9 (253 to 290)**	**<0.001**
Average minimum principal strain (μstrain)	**-622 ± 32 (-674 to -546)**	**-553 ± 29 (-596 to -550)**	**<0.001**

ATC, anatomical tibial component; STC, symmetric tibial component; SD, standard deviation.

*Minimum principal strain was expressed as a negative value.

*Bold, $p<0.05$.

Table 4 shows the correlation between the distance from the distal stem tip to the cortical bone and stress/strain measurements. ATC and STC showed a negative correlation between this distance and peak stress around the distal stem tip (ATC r=-0.459, p=0.014; STC r=-0.536, p=0.003). In the medial half of the

proximal tibial bone, ATC showed a positive correlation of distance with the average von Mises stress (r=0.434, p=0.021) and a negative correlation of distance with the average minimal principal strain (r=-0.417, p=0.027). STC showed no correlation between distance and average values in the medial half of the proximal tibial bone.

Table 4. Results of Pearson correlation between the distance from distal stem tip to cortical bone and stress/strain measurements

Correlation with distance	ATC		STC	
	r	p-value	r	p-value
Around stem tip area				
Peak von Mises stress	**-0.459**	**0.014**	**-0.536**	**0.003**
Medial half of proximal tibial bone				
Peak von Mises stress	0.044	0.825	0.166	0.400
Average von Mises stress	**0.434**	**0.021**	0.293	0.130
Average maximum principal strain	0.254	0.191	0.140	0.479
Average minimum principal strain	**-0.417**	**0.027**	-0.291	0.133

ATC, anatomical tibial component; STC, symmetric tibial component; SD, standard deviation.

*Bold, $p<0.05$.

The intra- and inter-observer reliabilities for the distance measurement were 0.975 and 0.872, respectively.

IV. DISCUSSION

Using FEA, we investigated whether the differences in implant design affect the distribution of stress and strain to periprosthetic bone. Although the stem of ATC was medialized, the distance to the shortest cortical bone in Korean women did not differ from that of STC due to the length and sagittal angle of the stem. When

the same body weight was applied to the FEM of Korean women, ATC had a lower peak stress on the distal stem tip and higher average strain and stress on the medial half of the proximal tibial bone compared to STC, which is more advantageous in preventing stress shielding. Therefore, the hypothesis that stress concentrations around the distal stem tip and reductions in the load on the proximal tibial bone were due to the medialized stem of ATC was rejected.

If new biomechanics different from the natural knee are formed after joint replacement surgery, the distribution of load around the implant is also changed. Changes in load distribution can further lead to changes in periprosthetic bone remodeling[9,18] and there is a risk of stress shielding in areas where the load is less than that of the natural knee. Subsequent periprosthetic bone loss can potentially affect implant stability and lead to mechanical failure[21]. The factors contributing to stress shielding after TKA have been divided into three main categories. First, surgical factors, including postoperative lower extremity alignment[22], rotational alignment of the tibial component[11], coronal alignment of the tibial component[23], mediolateral baseplate position[24], and the presence of underhang[8], can contribute to stress shielding and bone loss after TKA. Second, host factors, such as the presence of sclerotic bone[25] and bone mineral density[26], are also known to affect load distribution. Third are implant factors, such as material and design. Since body weight is transmitted to the tibia through the tibial component in TKA, differences in implant characteristics can directly impact load distribution. Since cobalt-chromium alloys have a higher modulus of elasticity than titanium alloys, stress shielding occurs more in the surrounding bone[6,12,27]; and the thicker the baseplate, the more likely bone loss will occur[7]. The shape of the component can also affect the distribution of load, which is related to the patient's anatomic geometry. As these various factors work together, most clinical studies analyzing the effect of implant design have found it impossible to control for other confounders. Therefore, in many previous studies, FEA was essential to evaluate the effect of implant factors. However, since most FEA studies have used one or

a small number of models, there is a limitation in that they do not reflect the anatomical diversity between patients. If only one FEM is used, determining the effect of different proximal tibial bone geometries for each patient would be impossible. Therefore, we implemented FEA to control for surgical and host factors and created 30 models to reflect the bony geometry of Koreans.

Contrary to expectations, there was no difference in the shortest distance to the anteromedial cortical bone between implants in spite of medialized stem of ATC. This was due to the difference in stem length and sagittal angle between stem axis and baseplate (Table 1). In ATC, the stem is biased 1.5 mm, while the distal stem tip is located proximally and anteriorly due to the short stem length and smaller sagittal angle (Fig. 5-A). Therefore, although the distal stem tip of ATC was located anteromedially compared to that of STC, there was no difference in the shortest distance since the anteromedial cortical bone had an oblique orientation (Fig. 5-B).

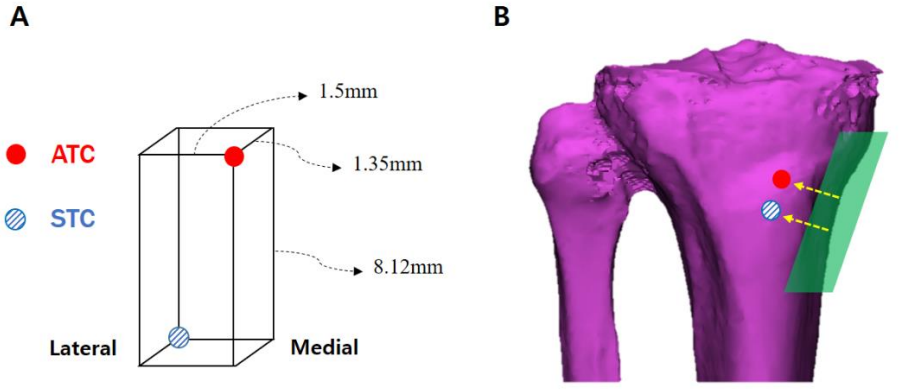

Figure 5. (A) Schematic composite image showing the positional relationship of the center point of the stem tip metal portion when ATC and STC are inserted with the same reference. (B) Due to the oblique orientation of anteromedial cortical bone, there is no difference in the shortest distance between two implants.

When each implant was inserted, there was a difference in the ratio of load distribution to the distal stem tip and the proximal cutting plane according to the design. Compared to STC, more stress and compressive strain (minimum principal strain) were applied to the proximal medial tibial bone in patients with ATC. This result can be explained by the following reasons. First, since the medial part of the ATC baseplate has a larger area than the lateral part, a relatively larger load is transferred to the medial half of the proximal tibial bone. Second reason may be the difference in overhang rates between implants. In the 3D simulation study of Ma *et al*., STC showed a higher overhang rate (42-48%) for the tibial cutting plane compared to ATC (3-7%)[28] when the implant was aligned along the medial 1/3 of tibial tubercle, as in our study. Since cortical bone is stiffer than cancellous bone and bears a lot of stress[29], more load is transferred to the cortical bone when the overhang occurs. In STC, a large load is distributed in the cortical bone of the lateral half of the proximal tibial bone, and a relatively smaller load is applied to the medial half of the cancellous bone.

As aforementioned, ATC shows more peak stress and compressive strain in the medial proximal tibial bone, which is more advantageous in preventing stress shielding in the relevant region[20,30]. This is contrary to the study by Cho *et al*., which showed more proximal medial tibial bone loss in ATC[5]. It can be also explained by the following two reasons. First, this study was implemented in an experimental setting which controlled the surgical and host factors. For example, in the multiple logistic regression analysis by Cho *et al*., when the fin of the proximal tibial stem was fitted to the medial sclerotic bone area, the odds of medial tibial bone loss were 3.79. However, since the existence of sclerotic bone was excluded in our simulation, the effect could not be analyzed. Therefore, ATC with a short stem, thin base plate, and efficient stress distribution may show the opposite result by sclerotic bone, which will be another topic for future research. Second, there was a difference in the stress/strain change of the proximal medial tibial bone according to the distance between the distal stem tip and the

anteromedial cortical bone. With ATC, as the distance decreased, the average von Mises stress and compressive strain of the medial half of the proximal tibial bone decreased. However, with STC, the distance and average stress/strain of the medial half of the proximal tibial bone were not correlated. Therefore, theoretically, if the distance is decreased due to large anatomical variations (e.g., severe proximal tibial bowing or large tibial shaft offset) or surgical errors (coronal alignment or mediolateral position), ATC is more likely to be negatively affected by stress transfer to the proximal tibial bone compared to STC. Also, the cortical rim of the proximal cutting plane involved in overhang affects stress distribution, and this may be one of the reasons why ATC has caused medial proximal tibial bone loss in actual clinical studies.

In previous FEA studies, stress and strain (or strain energy density) were used to predict bone resorption[20,24,31] of the periprosthetic bone. Since most of the studies utilize one or a limited number of FEMs, they try to predict bone resorption based on specific thresholds, but these values vary from study to study[9,30,32]. This is because bones respond differently to load depending on race, gender, age and situations. Therefore, our study obtained the average measurements of 30 Korean women, and tried to judge the possibility of bone resorption through statistical comparison, not based on a specific threshold. However, since it is not yet known whether the difference in the average measurements of the elements in the region of interest causes a difference in actual bone resorption, a longitudinal experimental study is required in the future.

Our study had several limitations. First, only Korean women were enrolled. Since the distribution of stress and strain according to the positional relationship between the implant and proximal tibial bone geometry was analyzed, the results may differ when targeting men[33,34] or other races[3] with different anatomy. Second, since every implant has a different design, our results cannot be generalized to other products. As the specifications for each implant can differ, it is likely to result in different stress distribution. Third, since the analysis was conducted in a

simulated experimental setting, the results may be different in *in vivo* settings wherein host and surgical factors are involved. However, this was also a strength of our research. The isolated biomechanical effect of implant design on Korean women was reported for the first time. Another strength of our study is that 30 FEMs were used differently from the previous FEA studies. This enabled our study to use statistical analysis and to reflect the anatomical diversity of Korean women.

V. CONCLUSION

Implant design, including medialized stem and the anatomic shape of the baseplate, affects the distribution of stress and strain on the proximal tibia. In Korean women, the medialized stem of ATC does not come closer to the cortical bone, contrary to concerns, and transmits more stress and strain to the proximal tibial bone compared to STC. However, unlike STC, the shorter the distance between the stem and the anteromedial cortical bone, the less stress and strain applied to the medial proximal cutting plane in ATC. Therefore, when using ATC, stress shielding should be considered in patients with severe anatomical variations or in cases of surgical error.

REFERENCES

1. Hicks CA, Noble P, Tullos H. The anatomy of the tibial intramedullary canal. Clin Orthop Relat Res 1995:111-6.
2. Abraham R, Malkani AL, Lewis J, Beck D. An anatomical study of tibial metaphyseal/diaphyseal mismatch during revision total knee arthroplasty. J Arthroplasty 2007;22:241-4.
3. Tang Q, Zhou Y, Yang D, Xu H, Liu Q. The offset of the tibial shaft from the tibial plateau in Chinese people. J Bone Joint Surg Am 2010;92:1981-7.
4. Yoo JH, Kang YG, Chang CB, Seong SC, Kim TK. The relationship of the medially-offset stem of the tibial component to the medial tibial cortex in total knee replacements in Korean patients. J Bone Joint Surg Br 2008;90:31-6.
5. Cho BW, Kwon HM, Hong YJ, Park KK, Yang IH, Lee WS. Anatomical tibial component is related to more medial tibial stress shielding after total knee arthroplasty in Korean patients. Knee Surg Sports Traumatol Arthrosc 2020; doi:10.1007/s00167-020-05869-x.
6. Martin JR, Watts CD, Levy DL, Kim RH. Medial Tibial Stress Shielding: A Limitation of Cobalt Chromium Tibial Baseplates. J Arthroplasty 2017;32:558-62.
7. Martin JR, Watts CD, Levy DL, Miner TM, Springer BD, Kim RH. Tibial Tray Thickness Significantly Increases Medial Tibial Bone Resorption in Cobalt-Chromium Total Knee Arthroplasty Implants. J Arthroplasty 2017;32:79-82.
8. Gu S, Kuriyama S, Nakamura S, Nishitani K, Ito H, Matsuda S. Underhang of the tibial component increases tibial bone resorption after total knee arthroplasty. Knee Surg Sports Traumatol Arthrosc 2019;27:1270-9.
9. Huiskes R, Weinans H, van Rietbergen B. The relationship between stress shielding and bone resorption around total hip stems and the effects of flexible materials. Clin Orthop Relat Res 1992:124-34.
10. Sumner DR. Long-term implant fixation and stress-shielding in total hip replacement. J Biomech 2015;48:797-800.
11. Kang K, Jang YW, Yoo OS, Jung D, Lee SJ, Lee MC, et al. Biomechanical Characteristics of Three Baseplate Rotational Arrangement Techniques in Total Knee Arthroplasty. Biomed Res Int 2018;2018:9641417.
12. Park HJ, Bae TS, Kang SB, Baek HH, Chang MJ, Chang CB. A three-dimensional finite element analysis on the effects of implant materials and designs on periprosthetic tibial bone resorption. PLoS One 2021;16:e0246866.
13. Doyle BJ, Morris LG, Callanan A, Kelly P, Vorp DA, McGloughlin TM. 3D reconstruction and manufacture of real abdominal aortic aneurysms:

from CT scan to silicone model. J Biomech Eng 2008;130:034501.
14. Kimpton CI, Crocombe AD, Bradley WN, Gavin Huw Owen B. Analysis of stem tip pain in revision total knee arthroplasty. J Arthroplasty 2013;28:971-7.
15. Morrison JB. The mechanics of the knee joint in relation to normal walking. J Biomech 1970;3:51-61.
16. Kutzner I, Bender A, Dymke J, Duda G, von Roth P, Bergmann G. Mediolateral force distribution at the knee joint shifts across activities and is driven by tibiofemoral alignment. Bone Joint J 2017;99-b:779-87.
17. Completo A, Rego A, Fonseca F, Ramos A, Relvas C, Simões JA. Biomechanical evaluation of proximal tibia behaviour with the use of femoral stems in revision TKA: an in vitro and finite element analysis. Clin Biomech (Bristol, Avon) 2010;25:159-65.
18. Frost HM. Wolff's Law and bone's structural adaptations to mechanical usage: an overview for clinicians. Angle Orthod 1994;64:175-88.
19. Pattin CA, Caler WE, Carter DR. Cyclic mechanical property degradation during fatigue loading of cortical bone. J Biomech 1996;29:69-79.
20. Huiskes R, Weinans H, Grootenboer HJ, Dalstra M, Fudala B, Slooff TJ. Adaptive bone-remodeling theory applied to prosthetic-design analysis. J Biomech 1987;20:1135-50.
21. Van Lenthe GH, de Waal Malefijt MC, Huiskes R. Stress shielding after total knee replacement may cause bone resorption in the distal femur. J Bone Joint Surg Br 1997;79:117-22.
22. Jaroma A, Soininvaara T, Kröger H. Periprosthetic tibial bone mineral density changes after total knee arthroplasty. Acta Orthop 2016;87:268-73.
23. Perillo-Marcone A, Barrett DS, Taylor M. The importance of tibial alignment: finite element analysis of tibial malalignment. J Arthroplasty 2000;15:1020-7.
24. Innocenti B, Truyens E, Labey L, Wong P, Victor J, Bellemans J. Can medio-lateral baseplate position and load sharing induce asymptomatic local bone resorption of the proximal tibia? A finite element study. J Orthop Surg Res 2009;4:26.
25. Li YR, Gao YH, Yang C, Ding L, Zhang X, Chen H, et al. Finite-element analysis of the proximal tibial sclerotic bone and different alignment in total knee arthroplasty. BMC Musculoskelet Disord 2019;20:617.
26. Shi M, Chen L, Wu H, Wang Y, Wang W, Zhang Y, et al. Effect of bisphosphonates on periprosthetic bone loss after total knee arthroplasty: a meta-analysis of randomized controlled trials. BMC Musculoskelet Disord 2018;19:177.
27. Yoon C, Chang MJ, Chang CB, Song MK, Shin JH, Kang SB. Medial Tibial Periprosthetic Bone Resorption and Its Effect on Clinical

Outcomes After Total Knee Arthroplasty: Cobalt-Chromium vs Titanium Implants. J Arthroplasty 2018;33:2835-42.

28. Ma Y, Mizu-Uchi H, Okazaki K, Ushio T, Murakami K, Hamai S, et al. Effects of tibial baseplate shape on rotational alignment in total knee arthroplasty: three-dimensional surgical simulation using osteoarthritis knees. Arch Orthop Trauma Surg 2018;138:105-14.
29. Osterhoff G, Morgan EF, Shefelbine SJ, Karim L, McNamara LM, Augat P. Bone mechanical properties and changes with osteoporosis. Injury 2016;47 Suppl 2:S11-20.
30. Frost HM. A 2003 update of bone physiology and Wolff's Law for clinicians. Angle Orthod 2004;74:3-15.
31. Jang IG, Kim IY, Kwak BB. Analogy of strain energy density based bone-remodeling algorithm and structural topology optimization. J Biomech Eng 2009;131:011012.
32. Christen P, Ito K, Ellouz R, Boutroy S, Sornay-Rendu E, Chapurlat RD, et al. Bone remodelling in humans is load-driven but not lazy. Nat Commun 2014;5:4855.
33. Lim HC, Bae JH, Yoon JY, Kim SJ, Kim JG, Lee JM. Gender differences of the morphology of the distal femur and proximal tibia in a Korean population. Knee 2013;20:26-30.
34. Cho BW, Nam JH, Koh YG, Min JH, Park KK, Kang KT. Gender-Based Quantitative Analysis of the Grand Piano Sign in Mechanically Aligned Total Knee Arthroplasty in Asians. J Clin Med 2021;10.

ABSTRACT(IN KOREAN)

인공슬관절전치환술에서 내측 근위 경골부의 응력차폐 현상에 해부학적 경골 치환물이 미치는 생체역학적 영향: 한국인 모델 30례 유한요소분석

<지도교수 박 관 규>

연세대학교 대학원 의학과

조 병 우

목적

본 연구는 유한요소분석법을 이용하여 한국인의 근위 경골의 응력분포에 해부학적 경골 치환물 (ATC)가 미치는 영향을 밝히는 것을 목적으로 한다.

재료 및 방법

10개의 절점을 가진 수정된 사면체 요소를 이용하여 30개의 경골의 3차원 유한요소모델을 생성하였다. 수술 시뮬레이션에는 대칭형 경골 치환물 (STC, NexGen LPS-Flex)과 ATC (Persona)가 사용되었다. 두 치환물의 원위스템부와 내측 근위 경골부에서 유한요소분석 측정치 (응력과 변형률), 원위 스템부에서 전내측 경골피질골까지의 거리를 구하여 통계적으로 비교하였다. 그리고 거리와 유한요소분석 측정치의 상관성을 분석하였다.

결과

스템 원위부에서 가장 가까운 전내측 경골피질골까지의 거리는 두 치환물간에 통계적 차이가 없었다. 하지만, 스템 원위부에서의 최대 응력은 STC가 ATC 보다 높았다. 내측 근위 경골부에서, 최대 응력은

두 치환물 간 통계적 차이가 없었다. 하지만 평균 응력, 평균 최대주변형률, 평균 최소주변형률은 ATC가 더 높았다. 두 치환물 모두 거리와 스템 원위부 주변 최대응력 사이에 음의 상관관계를 보였다. 내측 근위 경골부에서 ATC는 거리와 평균 응력간의 양의 상관관계, 거리와 평균 최소주변형률간에 음의 상관관계를 보였다. STC는 거리와 근위 내측 경골부의 유한요소분석 측정치들과 상관관계를 보이지 않았다.

결론

내측 전위스템, 베이스플레이트의 해부학적 형태를 포함한 치환물의 디자인은 근위 경골부의 응력과 변형률 분포에 영향을 미친다. 한국인 여성에서, ATC는 내측전위스템을 가지고있지만 STC에 비해서 스템 원위부가 전내측 경골피질골과 더 가깝지 않다. 그러나 ATC는 STC와 다르게 거리가 짧아질수록 내측 근위 경골부에 주어지는 응력과 변형률도 감소하게 된다. 따라서 ATC를 사용할 때 심한 해부학적 변형이 있는 환자나 수술 오류가 발생할 경우 응력 차폐의 가능성을 고려해야 한다.

핵심되는 말: 인공슬관절 전치환술, 유한요소분석, 해부학적 경골 치환물, 응력차폐 현상, 내측근위경골부 골 소실